

# Neutrino Oscillations and the Anomalous Atmospheric Neutrino Flux

K. Hidaka

*Department of Physics, Tokyo Gakugei University, Koganei, Tokyo 184, Japan*

M. Honda

*Institute for Cosmic Ray Research, University of Tokyo, Tanashi, Tokyo 188, Japan*

and

S. Midorikawa

*Institute for Nuclear Study, University of Tokyo, Tanashi, Tokyo 188, Japan*

(Received 24 June 1988)

We reanalyze the constraints on atmospheric  $\nu_e$  and  $\nu_\mu$  fluxes due to three-neutrino oscillations and investigate the anomalous neutrino fluxes recently observed at Kamiokande. We find that it is difficult to explain the data by  $\nu_e \leftrightarrow \nu_\mu$  oscillations alone. We also show that models of three neutrino flavors with neutrino-mass-squared differences of order  $10^{-2} \text{ eV}^2$  can solve both the solar and the atmospheric neutrino problems simultaneously.

PACS numbers: 94.40.-i, 12.15.Ff, 14.60.Gh, 96.60.Kx

The masses and mixing pattern of neutrinos are long-standing problems in particle physics.<sup>1</sup> In the light of this, the anomalous atmospheric neutrino fluxes recently observed at Kamiokande are very interesting.<sup>2</sup> While the number of electronlike single-prong events is in good agreement with the prediction of a Monte Carlo calculation, the number of muonlike single-prong events is  $(59 \pm 7)\%$  (statistical error) of the Monte Carlo prediction. In this Letter we investigate the possibility of explaining the data in terms of neutrino oscillations. We focus our attention on the compatibility of this explanation with the solar neutrino problem, and derive constraints on parameters such as the masses and mixing angles of neutrinos.

Let us consider a model of three neutrino flavors. For

simplicity we neglect the CP-violating phase. Weak eigenstates  $\nu_\alpha$  ( $\alpha = e, \mu, \tau$ ) are related with mass eigenstates  $\nu_i$  (mass  $m_i$ ) ( $i = 1, 2, 3$ ) by  $\nu_\alpha = V_{\alpha i} \nu_i$ , where

$$V = \begin{pmatrix} c_1 c_3 & s_1 c_3 & s_3 \\ -s_1 c_2 - c_1 s_2 s_3 & c_1 c_2 - s_1 s_2 s_3 & s_2 c_3 \\ s_1 s_2 - c_1 c_2 s_3 & -c_1 s_2 - s_1 c_2 s_3 & c_2 c_3 \end{pmatrix}, \quad (1)$$

$s_i = \sin \theta_i$  and  $c_i = \cos \theta_i$  ( $i = 1, 2, 3$ ). Without loss of generality we can impose a condition that the largest component of  $\nu_e$  is  $\nu_1$ , which is expressed by  $c_1^2 \geq \frac{1}{2}$  and  $s_3^2 \leq c_1^2 / (1 + c_1^2) \leq \frac{1}{2}$ .

The numbers  $N_\mu$  and  $N_e$  of the observed muon and electron events expected in the presence of oscillations are given by

$$N_\mu = \kappa \sum_{\nu, \bar{\nu}} \epsilon_\mu(E_\mu) \sigma_\mu(E_\nu, E_\mu) [F_\mu(E_\nu, \theta_\nu) P(\nu_\mu \rightarrow \nu_\mu) + F_e(E_\nu, \theta_\nu) P(\nu_e \rightarrow \nu_\mu)] dE_\mu dE_\nu d\theta_\nu, \quad (2)$$

$$N_e = \kappa \sum_{\nu, \bar{\nu}} \epsilon_e(E_e) \sigma_e(E_\nu, E_e) [F_\mu(E_\nu, \theta_\nu) P(\nu_\mu \rightarrow \nu_e) + F_e(E_\nu, \theta_\nu) P(\nu_e \rightarrow \nu_e)] dE_e dE_\nu d\theta_\nu,$$

where  $\kappa = (\text{number of nucleons}) \times (\text{time})$ ,  $\epsilon_\alpha(E_\alpha)$  is the detection efficiency for  $\alpha$ -type charged leptons with energy  $E_\alpha$ ,  $\sigma_\alpha$  is the differential cross section of  $\nu_\alpha$ ,  $F_\alpha(E_\nu, \theta_\nu)$  is the incident  $\nu_\alpha$  flux with energy  $E_\nu$  and zenith angle  $\theta_\nu$ , and  $P(\nu_\alpha \rightarrow \nu_\beta)$  is the time-averaged oscillation probability. We define

$$U_\mu = \frac{N_\mu}{\kappa \langle \epsilon_\mu \sigma_\mu F_\mu \rangle}, \quad U_e = \frac{N_e}{\kappa \langle \epsilon_e \sigma_e F_\mu \rangle}, \quad (3)$$

$$f_1 = \frac{\langle \epsilon_\mu \sigma_\mu F_e \rangle}{\langle \epsilon_\mu \sigma_\mu F_\mu \rangle}, \quad f_2 = \frac{\langle \epsilon_e \sigma_e F_e \rangle}{\langle \epsilon_e \sigma_e F_\mu \rangle},$$

where

$$\langle \epsilon_\alpha \sigma_\alpha F_\beta \rangle = \sum_{\nu, \bar{\nu}} \int \epsilon_\alpha(E_\alpha) \sigma_\alpha(E_\nu, E_\alpha) F_\beta(E_\nu, \theta_\nu) dE_\alpha dE_\nu d\theta_\nu.$$

Then Eq. (2) reduces to

$$U_\mu = P(\nu_\mu \rightarrow \nu_\mu) + f_1 P(\nu_e \rightarrow \nu_\mu), \quad (4)$$

$$U_e = f_2 P(\nu_e \rightarrow \nu_e) + P(\nu_\mu \rightarrow \nu_e).$$

Using the theoretical estimates of  $F_\mu$  and  $F_e$  for Kamioka,<sup>3</sup> the data of neutrino cross sections, and the detection efficiency of the detector,<sup>4</sup> we obtain  $\langle \epsilon_\mu \sigma_\mu F_\mu \rangle = 2.65$

$\times 10^{-39}$  (events/sec)/nucleon,  $\langle \epsilon_e \sigma_e F_\mu \rangle = 3.63 \times 10^{-39}$  (events/sec)/nucleon, and  $f_1 = f_2 = 0.44 \equiv f$ . The estimate of  $f_1$  and  $f_2$  has  $\leq 5\%$  error due to the theoretical uncertainty in the  $F_e/F_\mu$  ratio.<sup>2</sup> In the case of Kamiokande,  $\kappa = 5.45 \times 10^{40}$  nucleons sec (2.87 kton yr). Note that in the case where  $f_1 = f_2$  Eq. (4) is equivalent to the Eq. (4) of Ref. 5.

Using Eq. (4) with  $f_1 = f_2 = 0.44$  we derive the allowed region in the  $(U_e, U_\mu)$  plane in two typical cases.

**Case I.**—Three neutrino flavors have executed many oscillations before being detected. For a typical energy  $E_\nu \sim 200$  MeV and a typical minimum distance  $\sim 30$  km this corresponds to  $\delta m_{ij}^2 = |m_i^2 - m_j^2| \gtrsim 1.7 \times 10^{-2}$  eV<sup>2</sup> for all pairs  $1 \leq i < j \leq 3$ . This value is slightly lower than the current upper limit obtained from reactor experiments.<sup>6</sup> The oscillation probability is given by  $P(\nu_\alpha \rightarrow \nu_\beta) = \sum_{i=1}^3 V_{\alpha i}^2 V_{\beta i}^2$  in this case. The allowed region which is evaluated numerically is depicted in Fig. 1. We find that the allowed region is slightly larger than that obtained in Ref. 5 for the same value of  $f$ .

**Case II.**—Only one oscillation mode dominates the neutrino oscillations, i.e.,  $\delta m_{12}^2 \ll 7.7 \times 10^{-5}$  eV<sup>2</sup> and  $\delta m_{13}^2 \approx \delta m_{23}^2 \gtrsim 1.7 \times 10^{-2}$  eV<sup>2</sup> so that the mode corresponding to  $\delta m_{12}^2$  is frozen in the range of the Earth's radius. In this case the oscillation probability is given by

$$P(\nu_\alpha \rightarrow \nu_\beta) = \delta_{\alpha\beta} - 2V_{\alpha 3}^2(\delta_{\alpha\beta} - V_{\beta 3}^2).$$

The lower bound on  $U_\mu$  for  $f/2 \leq U_e \leq (1+f)/2$  is determined by

$$\begin{aligned} U_e &= f(1 - 2x + 2x^2) + 2z(1 - x), \\ U_\mu &= (1 - 2z + 2z^2) + 2fz(1 - x), \end{aligned} \quad (5)$$

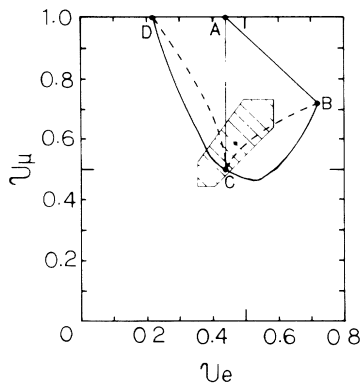


FIG. 1. Plots of  $U_\mu$  vs  $U_e$ . The value  $f$  is taken to be 0.44. The seven regions of interest are as follows. (i) The point A corresponds to no neutrino oscillations. (ii) The line AB corresponds to  $\nu_e \leftrightarrow \nu_\mu$  mixing. (iii) The line AC corresponds to  $\nu_\mu \leftrightarrow \nu_\tau$  mixing. (iv) The line AD corresponds to  $\nu_e \leftrightarrow \nu_\tau$  mixing. (v) The region ABCD (solid line) corresponds to three flavor mixing (case I). (vi) The region ABCD (dashed line) corresponds to three flavor mixing (case II). (vii) The region allowed by Eq. (7) is represented by the hatched area.

where

$$z = z_\pm \equiv \frac{1}{4} \{ [4fx + (1 - 2f)] \pm [-8f(1 - f)x + (1 + 4f - 4f^2)]^{1/2} \} \quad (6)$$

and  $\frac{1}{2} \leq x \leq 1$ . Here  $z = z_-$  for  $f/2 \leq U_e \leq f$ , and  $z = z_+$  for  $f \leq U_e \leq (1+f)/2$ . The lower bound is represented by the dashed line in Fig. 1. The upper bound is the same as that in case I.

From the Kamiokande data, we can deduce the values of  $U_e$ ,  $U_\mu$ , and  $U_e/U_\mu$ . Taking into account the statistical errors of the data, the theoretical uncertainty in the expected neutrino fluxes of  $\pm 20\%$ , and the experimental error in the neutrino cross sections of  $\pm 10\%$ , we obtain

$$\begin{aligned} U_e &= 0.470 \pm 0.116, \quad U_\mu = 0.588 \pm 0.146 \\ U_e/U_\mu &= 0.798 \pm 0.120, \end{aligned} \quad (7)$$

for momentum cuts of  $p_e > 100$  MeV/c and  $p_\mu > 205$  MeV/c. We plot the region allowed by Eq. (7) in Fig. 1. From this figure we find (i) that the point  $(U_e, U_\mu) = (f, 1)$  corresponding to no oscillations is excluded at the 99.5% C.L. and (ii) that it is possible to explain the Kamiokande data by the three-neutrino oscillations of both case I and case II. The quantity  $U_e + U_\mu$  provides the most stringent criterion for the two-neutrino oscillations  $\nu_e \leftrightarrow \nu_\mu$ . The line  $U_e + U_\mu = 1 + f = 1.44$  corresponds to the two-neutrino oscillations. From the data, we obtain  $U_e + U_\mu = 1.06 \pm 0.25$ . Thus the two-neutrino oscillations are excluded at the 87% C.L.

We can deduce the region of the mixing angles of Eq. (1) corresponding to Eq. (7). First we consider case I. We are interested in the compatibility of the solution

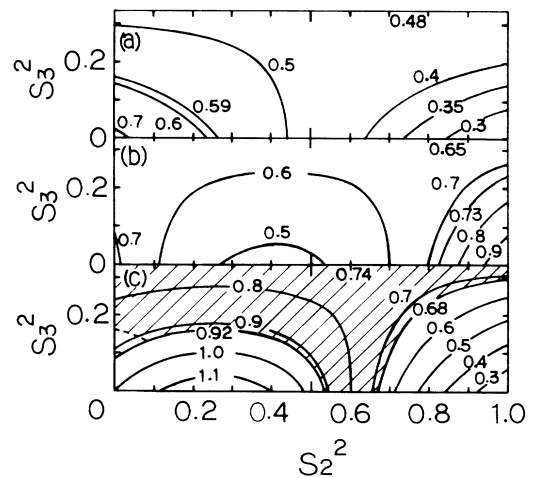


FIG. 2. (a) The iso- $U_e$ , (b) iso- $U_\mu$ , and (c) iso- $U_e/U_\mu$  contour plots in the  $(s_2^2, s_3^2)$  plane for the three-flavor-mixing model (case I) with  $s_1^2 = \frac{1}{2}$  for which  $s_3^2$  is restricted by the imposed condition  $s_3^2 \leq \frac{1}{3}$ . The region allowed by Eq. (7) is represented by the hatched area in (c).

with the solar neutrino problem.<sup>7,8</sup> As possible solutions to this problem with vacuum oscillations favor large mixing angles, it is reasonable to take  $\theta_1$  as  $45^\circ$  and find constraints on  $\theta_2$  and  $\theta_3$ . The iso- $U_e$ , iso- $U_\mu$ , and iso- $U_e/U_\mu$  contour plots with  $\theta_1 = 45^\circ$  are shown in Fig. 2, where the condition  $s_3^2 \leq \frac{1}{3}$  is imposed without loss of generality. The region allowed by Eq. (7) is represented in Fig. 2(c). Note that the region contains the  $s_3^2 = \frac{1}{3}$  line. For  $s_1^2 = \frac{1}{2}$  and  $s_3^2 = \frac{1}{3}$ , the average probability  $P(\nu_e \rightarrow \nu_e)$  takes its minimum value  $\frac{1}{3}$  which is marginally consistent with the ratio (observed solar  $\nu_e$  flux)/(predicted solar  $\nu_e$  flux). Hence solving both the atmospheric and solar neutrino problems simultaneously requires the angles  $\theta_1$  and  $\theta_3$  to take the values  $\theta_1 = 45^\circ$  and  $\theta_3 = 35.3^\circ$  almost uniquely. Here we note that there is no Mikheyev-Smirnov-Wolfenstein (MSW) effect<sup>9,10</sup> in the Earth on the atmospheric and solar neutrinos for  $\theta_1 = 45^\circ$ ,  $\theta_3 = 35.3^\circ$ , and  $\delta m_{ij}^2 \sim 10^{-2} \text{ eV}^2$ .

Case II is of particular interest for the compatibility with the solar neutrino problem which may possibly be solved by the MSW effect on  $\nu_e \leftrightarrow \nu_\mu$  or  $\nu_e \leftrightarrow \nu_\tau$  oscillations, since the condition  $\delta m_{12}^2 \ll 7.7 \times 10^{-5} \text{ eV}^2$  is compatible with the MSW region  $10^{-7} \text{ eV}^2 \lesssim \delta m_{12}^2 \lesssim 10^{-4} \text{ eV}^2$  in the two-generation model. In this case,  $U_e$  and  $U_\mu$  do not depend on  $\theta_1$ . In Fig. 3, we represent the iso- $U_e$ , iso- $U_\mu$ , and iso- $U_e/U_\mu$  contour plots in the  $(s_2^2, s_3^2)$  plane, where the condition  $s_3^2 \leq \frac{1}{2}$  is imposed. We also plot the region allowed by Eq. (7) in Fig. 3(c). A large

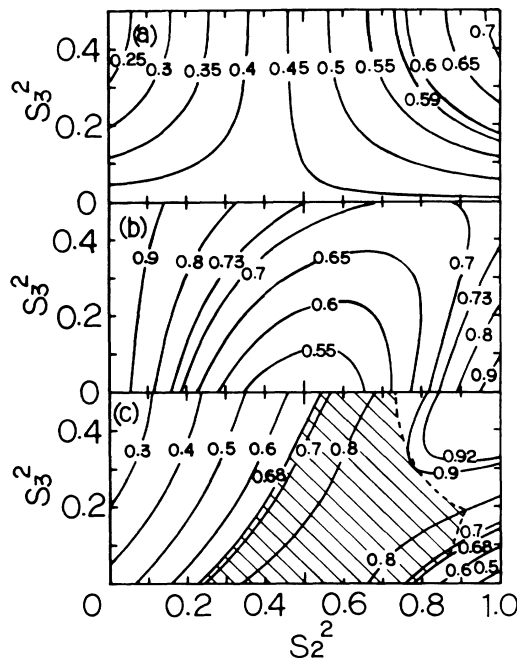


FIG. 3. (a) The iso- $U_e$ , (b) iso- $U_\mu$ , and (c) iso- $U_e/U_\mu$  contour plots in the  $(s_2^2, s_3^2)$  plane for the three-flavor-mixing model (case II) where  $s_3^2$  is restricted by the imposed condition  $s_3^2 \leq \frac{1}{2}$ . The region allowed by Eq. (7) is represented in (c) by the hatched area.

mixing angle  $\theta_2$  ( $28^\circ \leq \theta_2 \leq 73^\circ$ ) is required to explain the data, implying that  $\nu_\mu \leftrightarrow \nu_\tau$  oscillations play an important role in solving the atmospheric neutrino problem. In the three-generation model, the region in the  $(\delta m_{12}^2, \theta_1)$  plane that could solve the solar neutrino problem<sup>11</sup> is substantially larger than that in the two-generation model.<sup>12</sup> For example, consider one of the case-II solutions with  $m_1^2 \sim 0 \text{ eV}^2$ ,  $m_2^2 \sim 10^{-5} \text{ eV}^2$ , and  $m_3^2 \sim 10^{-2} \text{ eV}^2$  (which satisfy a condition  $m_1^2 \ll m_2^2 \ll m_3^2$ ), and  $-\pi/4 < \theta_3 < \pi/8$ . This three-generation model reduces to the effective two-generation model,<sup>11</sup> which ensures the compatibility of our atmospheric neutrino solution with the solar neutrino problem.

We have found possible solutions of the atmospheric and solar neutrino problems in terms of neutrino oscillations. One of them (case I) resolves the solar neutrino problem by the vacuum oscillations, and the other (case II) by the MSW effect. Both solutions assume that the largest of the  $\delta m^2$ 's is of order  $\sim 10^{-2} \text{ eV}^2$ , which is not excluded by current laboratory experiments. If this is the case, the oscillation effect will cease for high-energy neutrinos with  $E_\nu \gtrsim 100 \text{ GeV}$ . The observed flux of upward-going muons produced by high-energy neutrinos ( $\langle E_\nu \rangle \sim 100 \text{ GeV}$ ) is consistent with theoretical predictions of no oscillations.<sup>13</sup> Therefore high- and low-energy atmospheric neutrino fluxes can be explained consistently by assuming the neutrino-mass-squared differences of order  $\sim 10^{-2} \text{ eV}^2$ .

After completing this work, we received other papers on this topic.<sup>14</sup>

We are grateful to J. Arafune, H. Suda, Y. Totsuka, Y. Oyama, M. Takita, and H. Terazawa for many helpful discussions. We also thank P. G. Edwards for his careful reading of the manuscript. One of us (S.M.) thanks the Iwanami Fujukai Foundation for financial aid.

<sup>1</sup>See for example, S. M. Bilenky and B. Pontecorvo, Phys. Rep. **41**, 225 (1978).

<sup>2</sup>K. S. Hirata *et al.*, Phys. Lett. B **205**, 416 (1988).

<sup>3</sup>T. K. Gaisser, T. Stanev, S. A. Bludman, and H. Lee, Phys. Rev. Lett. **51**, 223 (1983); T. K. Gaisser, T. Stanev and G. Barr, Phys. Rev. D **38**, 85 (1988).

<sup>4</sup>M. Takita, private communication.

<sup>5</sup>P. H. Frampton and S. L. Glashow, Phys. Rev. D **25**, 1982 (1982).

<sup>6</sup>V. Zacek, in *Proceedings of the Twenty Third International Conference on High Energy Physics, Berkeley, California, July 16-23, 1986*, edited by S. L. Loken (World Scientific, Singapore 1986), Vol. 2, p. 903; F. Boehm, in *Proceedings of the Twelfth International Conference on Neutrino Physics and Astrophysics, Sendai, 1986*, edited by T. Kitagaki and H. Yuta (World Scientific, Singapore, 1986), p. 135.

<sup>7</sup>R. Davis, in *Proceedings of the Seventh Workshop on Grand Unification/ICOBAN'86*, edited by J. Arafune (World Scientific, Singapore, 1987), p. 237.

<sup>8</sup>N. Bahcall and R. K. Ulrich, Rev. Mod. Phys. **60**, 297 (1988).

<sup>9</sup>S. P. Mikheyev and A. Yu. Smirnov, *Yad. Fiz.* **42**, 1441 (1985) [*Sov. J. Nucl. Phys.* **42**, 913 (1985)].

<sup>10</sup>L. Wolfenstein, *Phys. Rev. D* **17**, 2369 (1978).

<sup>11</sup>T. K. Kuo and J. Pantaleone, *Phys. Rev. D* **35**, 3432 (1987); C. W. Kim and W. K. Sze, *Phys. Rev. D* **35**, 1404 (1987); C. S. Lim, in *Proceedings of the Brookhaven National Laboratory Neutrino Workshop*, Upton, New York, 5-7 February 1987 (to be published).

<sup>12</sup>H. A. Bethe, *Phys. Rev. Lett.* **56**, 1305 (1986); S. P. Rosen and J. M. Gelb, *Phys. Rev. D* **34**, 969 (1986); S. J. Parke, *Phys. Rev. Lett.* **57**, 1275 (1986); S. J. Parke and T. P. Walker, *Phys. Rev. Lett.* **57**, 2322 (1986).

<sup>13</sup>Y. Oyama, private communication.

<sup>14</sup>J. Learned, S. Pakvasa, and T. Weiler, *Phys. Lett. B* **207**, 79 (1988); V. Barger and K. Whisnant, Wisconsin University, Madison, Report No. MAD/PH/414 (to be published).